# AN INTEGRATED SIMULATION MODEL FOR SAND PRODUCTION PREDICTION AND SAND CONTROL

Ariffin Samsuri[1], Sim Soon Hin[2], Tan Czek Hoong[3]
Faculty of Chemical Engineering and Natural Resources Engineering
Universiti Teknologi Malaysia
81310, Johor Bahru.
Tel : 07-5502372[1], 012-7158773[3] Fax : 07-5581463
Email : ariffin@rmc.utm.my[1], simsoonhin@hotmail.com[2], amon530@hotmail.com[3]

## ABSTRACT

The paper describes the development of a computer package that can be used to predict sand production and select the optimum sand control. This package consists of two major parts. The first is simulation of perforation stability and onset of sand production. This is a coupled mechanical and fluid flow model. The main objectives of this model are predicting the onset of sand production, study the effect of perforation pattern, perforation density, phasing angle and 2-phase fluid (oil and water) production on the perforation cavity stability. The finite element method is used to develop this model. Among the assumptions made were that the reservoir rock surrounding the perforation cavity is assumed isothermal with its pores completely filled with fluid. The oil and water either in perforation cavity or in pores are considered totally immiscible. The deformation condition is considered nonlinear. The perforation boundary that is in contact with cement is assumed to be under no flow and displacement condition.

In the events that sand production cannot be avoided, gravel packing is normally carried out to prevent the sand from entering the wellbore. This causes decline in well productivity, which is characterized by the additional pressure drop across the well. The productivity impairment is often aggravated by high-velocity flow. A finite-difference model is developed to evaluate the productivity of gravel-packed wells. This is the second part of the computer package and it represents an improved approach to the study of production impairment due to gravel-packing compared to the current practice of using the skin concept. In this work, the perforations are treated as cylinders and the annulus between the perforation and screen is filled with gravel.

## DEVELOPMENT OF NUMERICAL MODEL

### The Perforation Stability Prediction Model

The perforation stability prediction model is comprised of 2 main elements: flow continuity equation (for oil and water phase) and solid equilibrium equation. The flow continuity equations determine the fluid pressure distribution around perforation cavity for a given set of boundary conditions. While the solid equilibrium equation with the fluid pressure evaluated by flow continuity equation, calculate stress state, elastic deformation and plastic deformation. According to Lewis and Schrefler (1987), the flow continuity equation is:

$$-\nabla^T\left\{\mathbf{k}\frac{k_{r_l}}{\mu_l B_l}\nabla(p_l+\rho_l gh)\right\}+\lambda_A\frac{\partial p_o}{\partial t}+\lambda_B\frac{\partial p_w}{\partial t}+\frac{S_l}{B_l}\left(\mathbf{m}^T-\frac{\mathbf{m}^T\mathbf{D}_T}{3K_s}\right)\frac{\partial\varepsilon}{\partial t}=0 \qquad (1)$$

The solid equilibrium equation can be written as:

$$\int_\Omega\delta\varepsilon^T\mathbf{D}_T\frac{\partial\varepsilon}{\partial t}d\Omega+\int_\Omega\delta\varepsilon^T\left(\frac{\mathbf{D}_T\mathbf{m}}{3K_s}-\mathbf{m}\right)\overline{SO}\frac{\partial p_o}{\partial t}d\Omega+\int_\Omega\delta\varepsilon^T\left(\frac{\mathbf{D}_T\mathbf{m}}{3K_s}-\mathbf{m}\right)\overline{SW}\frac{\partial p_w}{\partial t}d\Omega$$
$$-\int_\Omega\delta\varepsilon^T\mathbf{D}_T\frac{\partial\varepsilon_o}{\partial t}d\Omega-\int_\Omega\delta\mathbf{u}^T\frac{d\mathbf{b}}{dt}d\Omega-\int_\Gamma\delta\mathbf{u}^T\frac{d\hat{\mathbf{t}}}{dt}d\Gamma=0 \qquad (2)$$

The $\mathbf{D}^T$ in equations (1) and (2) is tangential stiffness matrix which is defined by constitutive model. It can be tangential elastic stiffness matrix, $\mathbf{D}^e$ for elastic deformation or tangent elastoplastic modulus matrix $\mathbf{D}^{ep}$ for plastic deformation. Two types of constitutive models that have been identified suitable to predict perforation cavity failure are available in the model. They are Mohr-Coulomb yield surface and Drucker-Prager yield surface (Veeken et al., 1991; Brady, 1994).

**3-D Flow Model for Sand Control Optimization**

The governing equation for this model is essentially a flow continuity equation in three-dimensional cylindrical co-ordinates (r,θ,z), that is

$$\frac{1}{r}\frac{\partial}{\partial r}\left[r\delta_r\lambda R\left(\frac{\partial P}{\partial r}-\gamma\frac{\partial h}{\partial r}\right)\right]+\frac{1}{r^2}\frac{\partial}{\partial\theta}\left[\delta_\theta\lambda\theta\left(\frac{\partial P}{\partial\theta}-\gamma\frac{\partial h}{\partial\theta}\right)\right]+\frac{\partial}{\partial z}\left[\delta_z\lambda Z\left(\frac{\partial P}{\partial z}-\gamma\frac{\partial h}{\partial z}\right)\right]=\Psi\frac{\partial P}{\partial t}+q \qquad (7)$$

The governing equation is discretized in space in the directions of r, θ and z for both the oil and water phases. The governing equation is also discretized in time into timesteps Δt, such that numerical solutions are sought on discrete time levels, i.e. $t_o=0$, $t_1=\Delta t,\ldots,t_n=n\Delta t$. The time discretization is accomplished by the forward difference approach. In this work, the distinction between the perforation and the reservoir rock is in their permeability only. Finally, the IMPES (Implicit Pressure Explicit Saturation) method is used to combine the governing equations for the oil and water phases. The difference equations are written for each grid block and the resulting system of equations is collected and expressed in matrix form as

$$\mathbf{AP}=\mathbf{D} \qquad (8)$$

where **A** is a the coefficient matrix, **P** is the solution matrix and **D** is a matrix of values which are constant at a particular timestep. Equation 8 is solved using the iterative Gauss-Seidel method for the pressure at the innermost part of the perforation, i.e. $P_p$. It is important to note that perforation here refers to the part of the perforation outside the casing. The pressure drop across this zone, $\Delta P_1$, is the difference between $P_r$ and $P_p$, i.e.

$$\Delta P_1=P_r-P_p \qquad (9)$$

**High-velocity flow effects**

As the flow velocity increases, deviations from Darcy's Law are observed which means that the law no longer applies. In this study, the Forchheimer equation is used in place of the Darcy Law in the modeling equations. The Forchheimer equation is given as follows,

$$u = -\delta \frac{k}{\mu} \frac{dp}{dx} \tag{10}$$

The symbol $\delta$ is a turbulence correction factor where $\delta = \frac{1}{\left(1 + \frac{\beta \rho k}{\mu}|u|\right)}$ and this is introduced into the governing equation in the manner shown in Eq. 7.

**Pressure drop in the casing-cement perforation tunnel**

In this work, the perforation is divided into two sections. The first is the perforation outside the casing, which has been discussed in the previous section. The second is a shorter tunnel in the both the casing and the cement. Due to its relatively small size, the flow regime in this tunnel is regarded as linear. The equation for linear one-dimensional flow through a perforation is given by Saucier as

$$\Delta P_2 = 0.888 \frac{L \mu q}{kA} + 9.1 \times 10^{-13} \beta L \rho \left(\frac{q}{A}\right)^2 \tag{11}$$

The first term on the right-hand side gives the pressure drop due to Darcy flow and the second term represent the additional pressure drop due to high-velocity flow.

## RESULTS AND DISCUSSION

The applicability of the package is demonstrated by running a sample case. The sample model is a circular reservoir containing oil only. It is delineated on the outside, top and bottom by no-flow boundaries. Fluid production is constant and both cases of openhole and perforation flow were considered. Various timestep sizes were used and the maximum simulation time was one (1) day. Relevant data of the model are as follows:

**Model Data**

Model outer radius : 1.524 m
Wellbore radius : 0.1524 m
Model height : 0.3048 m
Porosity : 25%
Perforation length : 0.1920 m (7.56 in.)
Perforation diameter : 0.0635 m (2.5 in.)
Number of perforation: 1 (Note: 0 for openhole case)
Gravel permeability : $1.9738 \times 10^{-6}$ $m^2$ (2000 mD)
Absolute permeability: $1.9738 \times 10^{-7}$ $m^2$ (200 mD)
Initial pressure : $1.3790 \times 10^{7}$ $m^2$ (2000 psi)

Young's Modulus : $0.1930 \times 10^{11}$ Pa
Poisson Ratio : 0.38
Friction Angle : $20^o$
Overburden : $1.8190 \times 10^{7}$ Pa
Horizontal Stress : $1.6175 \times 10^{7}$ Pa

**Oil Properties Table**

| Pressure (Pa) | 1/Bo | viscosity | density |
|---|---|---|---|
| 1.448E+07 | 0.716 | 0.230E-2 | 8.500E+02 |
| 1.276E+07 | 0.734 | 0.230E-2 | 8.500E+02 |
| 1.103E+07 | 0.751 | 0.230E-2 | 8.500E+02 |
| 9.308E+06 | 0.769 | 0.230E-2 | 8.500E+02 |
| 7.584E+06 | 0.786 | 0.230E-2 | 8.500E+02 |
| 5.861E+06 | 0.803 | 0.230E-2 | 8.500E+02 |
| 4.137E+07 | 0.822 | 0.230E-2 | 8.500E+02 |
| 2.413E+07 | 0.847 | 0.230E-2 | 8.500E+02 |

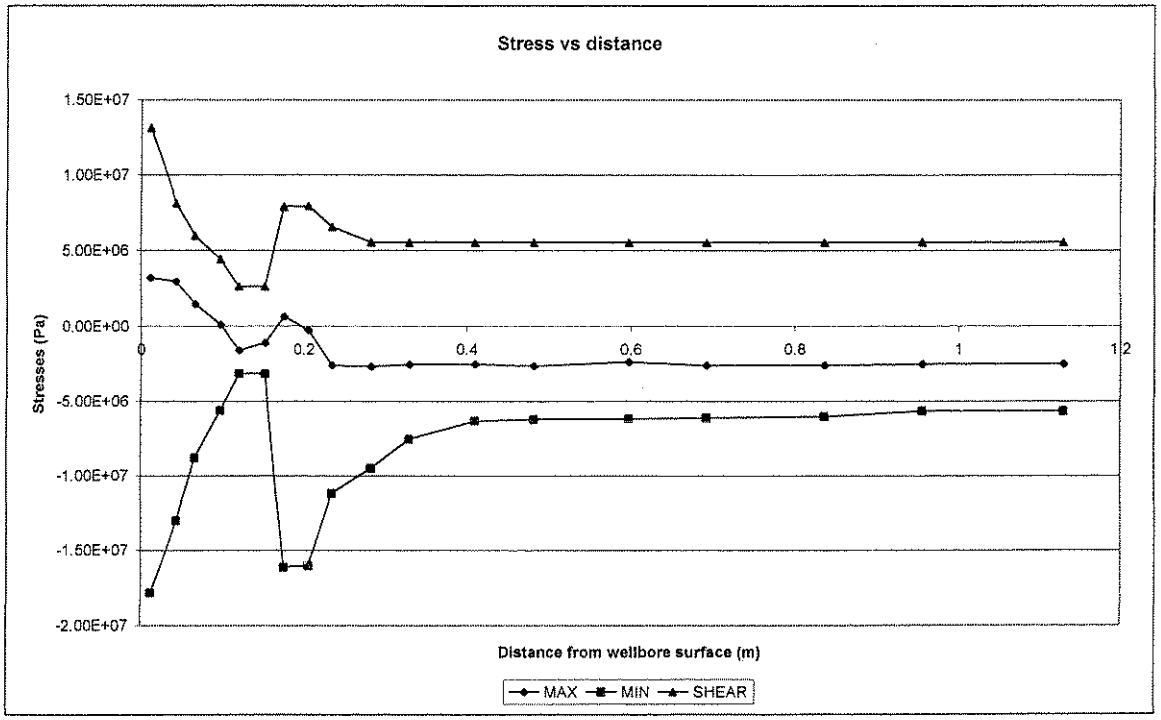


**Fig. 1: Stress distribution in the wellbore**

Fig. 1 shows the stress distribution along the upper element of perforation. It indicates that the highest shear stress and minimum principle stress always occurred at the Gauss point closest to the wellbore and the second peak was at the Gauss point adjacent to the perforation tips. It also shows that the perforation was always surrounded by high stress concentration the stress concentration decreased moving away from the perforation.

The effect of perforation (and gravel packing) on the flow performance is given by the following plot of pressure versus distance from the wellbore (Fig. 2). The openhole case consistently registered a higher pressure than the perforated case at all intervals. This also indicated a higher drawdown for the perforated case for the same flow rate. This in fact represented some performance impairment for the perforated case,

which agrees with previous studies using skin factors. The decline in productivity can also be seen in terms of the additional pressure drop that occurred, which is simply the pressure difference of the openhole and perforated model, or 20.35 psi in this case.

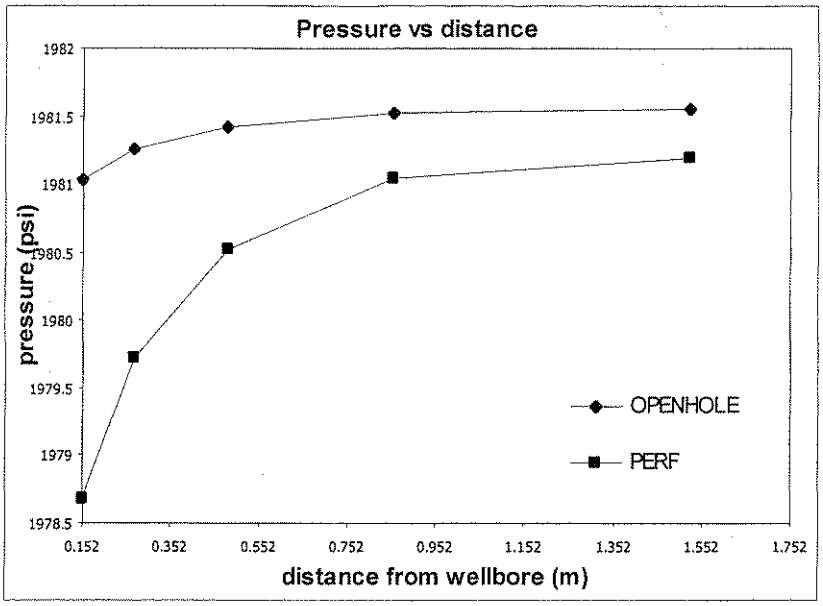


**Fig. 2: Pressure versus distance from wellbore**

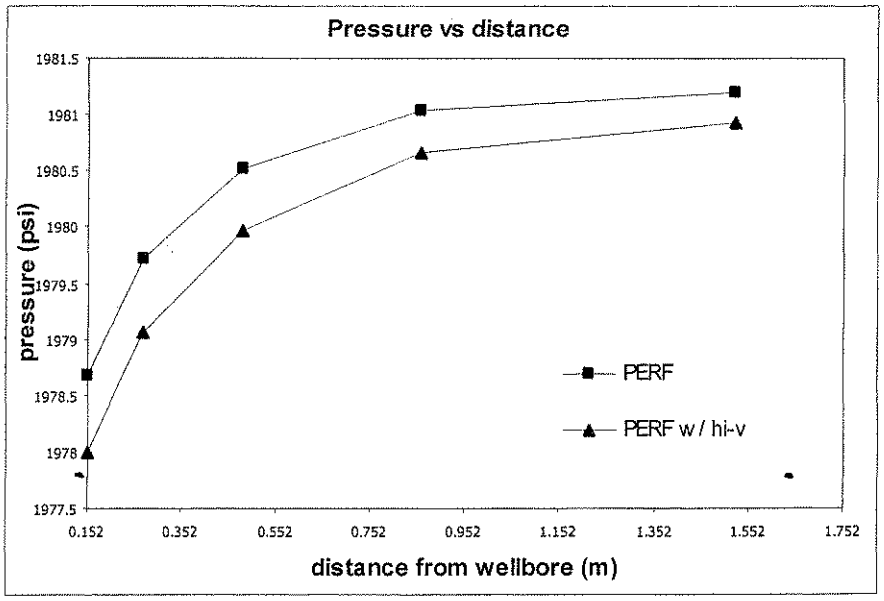


**Fig. 3: Pressure versus distance from wellbore**

$\theta_0$ - angular stress invariant
$\rho$ - density
$\Gamma$ - boundary
$\Omega$ - domain
u - fluid velocity, ft/s
$\delta$ - turbulence factor, dimensionless
$\Psi$ - $\frac{\varphi}{B}$, dimensionless
q - mass flow rate, lbm/s
t - time, s
**A** - coefficient matrix
**P** - solution matrix
**D** - matrix of constant values
$\beta$ - high-velocity $\beta$ coefficient, $md^{-1}$
L - length of casing-cement perforation tunnel, ft
A - flow area of perforation tunnel, $ft^2$
$\Delta P_1$ - pressure drop across reservoir, psi
$\Delta P_2$ - pressure drop in casing-cement perforation tunnel, psi

Subscript
o - oil phase
w - water phase
r - in r direction
$\theta$ - in $\theta$ direction
z - in z direction

Superscript
T - matrix transpose

**REFERENCE**

1. Aziz, K., Settari, A. (1979). "Petroleum Reservoir Simulation." Elsevier Applied Science.
2. Brady, B.H. (1994). "Some Recent Advances in Computational Geomechanics for Energy Resource Recovery." Computer Methods and Advances in Geomechanics, Siriwardane and Zaman (eds), Balkema Rotterdam. 21-31.
3. Golan, M., Whitson, C.H. (1991). "Well Performance." *Second Edition*, Prentice-Hall Inc., New Jersey.
4. Lewis, R.W. and Schrefler, B.A. (1987). "The Finite Element Method in the Deformation and Consolidation of Porous Media." Chichester: John Wiley and Sons.
5. Unneland, T. (2001) "Performance of High-Rate Gravel-packed Oil Wells" Dr. Techn. Thesis, Norwegian University of Science and Technology.
6. Veeken, C.A.M., Davies, D.R., Kenter, C.J. and Kooijman, A.P. (1991). "Sand Production Prediction Review: Developing an Integrated Approach." SPE 22792.